3D Multispecies Nonlinear Perturbative Particle Simulations of Collective Instabilities in Intense Particle Beams[1]

Hong Qin, Ronald C. Davidson, and W. Wei-li Lee

Princeton Plasma Physics Laboratory
Princeton University

PPPL
PRINCETON PLASMA
PHYSICS LABORATORY

[1]Work supported by U.S. Department of Energy and the Short Pulse Spallation Source Project and LANSCE Division of LANL.

Motivation

- Study collective instabilities in high-intensity ion beams for applications to:
  - Spallation neutron sources.
  - Heavy ion fusion.
  - Hadron colliders.

- 3D multi-species nonlinear δf particle simulation code provides an effective tool for investigating the following processes:
  - Electron-ion two-stream instability.
  - Periodically-focused equilibrium solutions in alternating-gradient focusing fields.
  - Dynamics of rms beam radius and other statistically averaged quantities.
  - Halo formation.

Theoretical Model

- Thin, continuous, high-intensity ion beam ($j = b$) propagates in the z-direction through background electron and ion components ($j = e, i$) described by distribution function $f_j(\boldsymbol{x}, \boldsymbol{p}, t)$.

- Transverse and axial particle velocities in a frame of reference moving with axial velocity $\beta_j c\hat{\mathbf{e}}_z$ are assumed to be *nonrelativistic*.

- Adopt a *smooth-focusing* model in which the focusing force is described by

$$\boxed{\boldsymbol{F}_j^{foc} = -\gamma_j m_j \omega_{\beta j}^2 \boldsymbol{x}_\perp}$$

- Self-electric and self-magnetic fields are expressed as $\boldsymbol{E}^s = -\nabla\phi(\boldsymbol{x}, t)$ and $\boldsymbol{B}^s = \nabla \times A_z(\boldsymbol{x}, t)\hat{\mathbf{e}}_z$.

- For perturbations with long axial wavelength ($k_z^2 r_b^2 \ll 1$), neglect the perturbed axial force on the charge components.

Theoretical Model

- Distribution functions and electromagnetic fields are described self-consistently by the nonlinear Vlasov-Maxwell equations in the six-dimensional phase space $(\boldsymbol{x}, \boldsymbol{p})$:

$$\boxed{\left\{\frac{\partial}{\partial t} + \boldsymbol{v}\cdot\frac{\partial}{\partial \boldsymbol{x}} - [\gamma_j m_j \omega_{\beta j}^2 \boldsymbol{x}_\perp + e_j(\nabla\phi - \beta_j \nabla_\perp A_z)]\cdot\frac{\partial}{\partial \boldsymbol{p}}\right\} f_j(\boldsymbol{x},\boldsymbol{p},t) = 0}$$

and

$$\boxed{\begin{aligned} \nabla^2\phi &= -4\pi\sum_j e_j \int d^3\boldsymbol{p} f_j(\boldsymbol{x},\boldsymbol{p},t) \\ \nabla^2 A_z &= -4\pi\sum_j e_j\beta_j \int d^3\boldsymbol{p} f_j(\boldsymbol{x},\boldsymbol{p},t) \end{aligned}}$$

PPPL PRINCETON PLASMA PHYSICS LABORATORY

Nonlinear δf Particle Simulation Method

- Divide the distribution function into two parts: $f_j = f_{j0} + \delta f_j$.
- f_{j0} is a known solution to the nonlinear Vlasov-Maxwell equations.
- Determine numerically the evolution of the perturbed distribution function $\delta f_j \equiv f_j - f_{j0}$.
- Advance the weight function defined by $w_j \equiv \delta f_j / f_j$, together with the particles' positions and momenta.
- Equations of motion for the particles are given by

$$\boxed{\begin{aligned} \frac{d\boldsymbol{x}_{ji}}{dt} &= (\gamma_j m_j)^{-1} \boldsymbol{p}_{ji} \\ \frac{d\boldsymbol{p}_{ji}}{dt} &= -\gamma_j m_j \omega_{\beta j}^2 \boldsymbol{x}_{\perp ji} - e_j(\nabla\phi - \beta_j \nabla_\perp A_z) \end{aligned}}$$

- Weight functions w_j are carried by the simulation particles, and the dynamical equations for w_j are derived from the definition of w_j and the Vlasov equation.

Nonlinear δf Particle Simulation Method

- Weight functions evolve according to

$$\boxed{\begin{aligned} \frac{dw_{ji}}{dt} &= -(1-w_{ji})\frac{1}{f_{j0}}\frac{\partial f_{j0}}{\partial \boldsymbol{p}}\cdot\delta\Big(\frac{d\boldsymbol{p}_{ji}}{dt}\Big) \\ \delta\Big(\frac{d\boldsymbol{p}_{ji}}{dt}\Big) &\equiv \frac{d\boldsymbol{p}_{ji}}{dt}\bigg|_{(\phi,A_z)\longrightarrow(\delta\phi,\delta A_z)} \end{aligned}}$$

Here, $\delta\phi = \phi - \phi_0$, $\delta A_z = A_z - A_{z0}$, and $(\phi_0,\ A_{z0},\ f_{j0}\ )$ are the equilibrium solutions.

- The perturbed distribution function δf_j is given by the weighted Klimontovich representation

$$\boxed{\delta f_j = \frac{N_j}{N_{sj}}\sum_{i=1}^{N_{sj}} w_{ji}\delta(\boldsymbol{x}-\boldsymbol{x}_{ji})\delta(\boldsymbol{p}-\boldsymbol{p}_{ji})}$$

where N_j is the total number of actual j'th species particles, and N_{sj} is the total number of *simulation* particles for the j'th species.

Nonlinear δf Particle Simulation Method

➪ Maxwell's equations are also expressed in terms of the perturbed quantities:

$$\boxed{\begin{aligned}
\nabla^2 \delta\phi &= -4\pi \sum_j e_j \delta n_j \\
\nabla^2 \delta A_z &= -4\pi \sum_j e_j \beta_j \delta n_j \\
\delta n_j &= \int d^3\boldsymbol{p}\, \delta f_j(\boldsymbol{x}, \boldsymbol{p}, t) = \frac{N_j}{N_{sj}} \sum_{i=1}^{N_{sj}} w_{ji} U(\boldsymbol{x}, \boldsymbol{x}_{ij})
\end{aligned}}$$

where $U(\boldsymbol{x}, \boldsymbol{x}_{ij})$ represents the method of distributing particles on the grids.

Advantages of the δf method

- Simulation noise is reduced significantly.
  - Statistical noise $\sim 1/\sqrt{N_s}$.
  - To achieve the same accuracy, number of simulation particles required by the δf method is only $(\delta f/f)^2$ times of that required by the conventional PIC method.
- No waste of computing resource on something already known — f_0.
- Moreover, make use of the known (f_0) to determine the unknown (δf).
- Study physics effects separately, as well as simultaneously.
- Easily switched between linear and nonlinear operation.

The BEST Code

Implementation of the 3D multispecies nonlinear δf simulation method described above is embodied in the Beam Equilibrium Stability and Transport (BEST) code at the Princeton Plasma Physics Laboratory.

- Advances the particle motions using a 4th-order Runge-Kutte method.
- Solves Maxwell's equations by a fast Fourier transform and finite-difference method in cylindrical geometry.
- Written in Fortran 90/95, the code utilizes extensively the object-oriented features provided by the computer language.
- The NetCDF scientific data format is implemented for large-scale diagnostics and visualization.
- The code has achieved an average speed of $40\mu s/(\text{particle}\times\text{step})$ on a DEC alpha personal workstation 500au computer.

Nonlinear Properties of Thermal Equilibrium Beams

- Single-species thermal equilibrium ion beam in a constant focusing field.
- Equilibrium properties depend on the radial coordinate $r = \sqrt{(x^2 + y^2)}$.
- Cylindrical chamber with perfectly conducting wall located at $r = r_w$.
- Thermal equilibrium distribution function for the beam ion is given by

$$f_{b0}(r, \boldsymbol{p}_\perp) = \frac{\hat{n}_b}{2\pi\gamma_b m_b T_b} \exp\left\{-\frac{p_\perp^2/2\gamma_b m_b + \gamma_b m_b \omega_{\beta b}^2 r^2/2 + e_b(\phi_0 - \beta_b A_{z0})}{T_b}\right\}$$

- System parameters are chosen to be: $\gamma_b = 1.85$, and normalized beam intensity $K\beta_b c\tau_\beta/\epsilon_0 = 0.025$, where $K = 2N_b e^2/\gamma_b^3 m_b \beta_b^2 c^2$ is the self-field perveance, and N_b is the number of beam ions per unit axial length. Normalized perpendicular beam temperature $T_b/\gamma_b m_b V_b^2 = 2.25 \times 10^{-6}$.

Nonlinear Properties of Thermal Equilibrium Beams

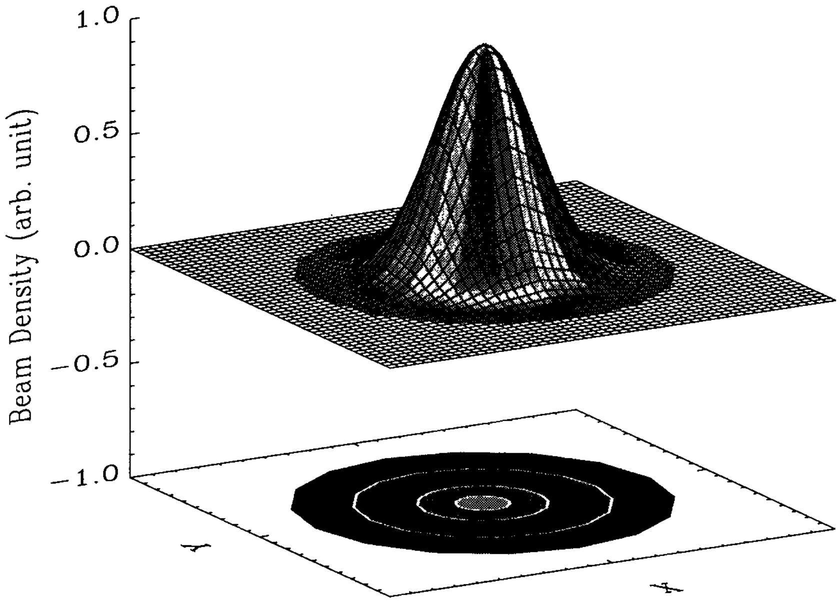

(a) Equilibrium Density

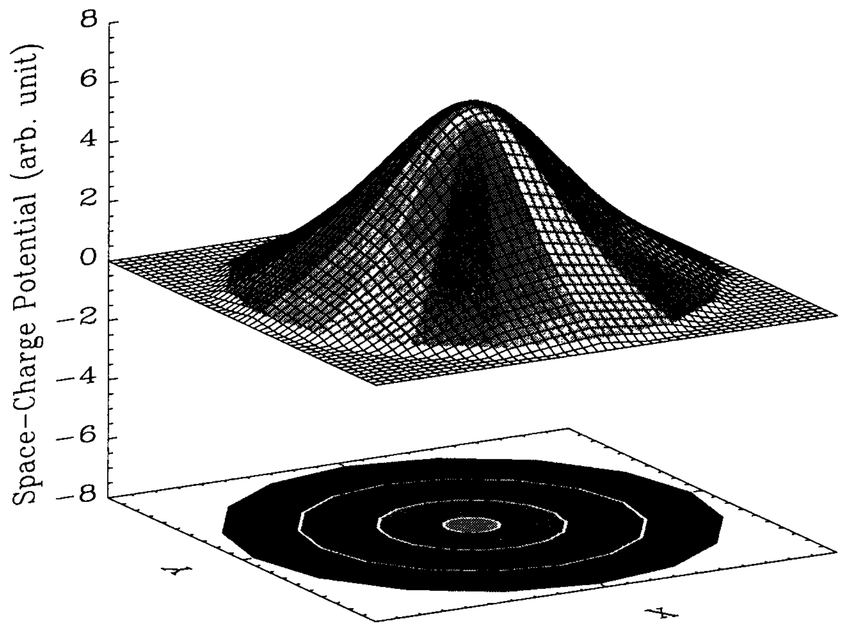

(b) Equilibrium Space-Charge Potential

➪ Equilibrium solutions (ϕ_0, A_{z0}, f_{j0}) solve the steady-state ($\partial/\partial t = 0$) Vlasov-Maxwell equations with $\partial/\partial z = 0$ and $\partial/\partial\theta = 0$.

Nonlinear Properties of Thermal Equilibrium Beams

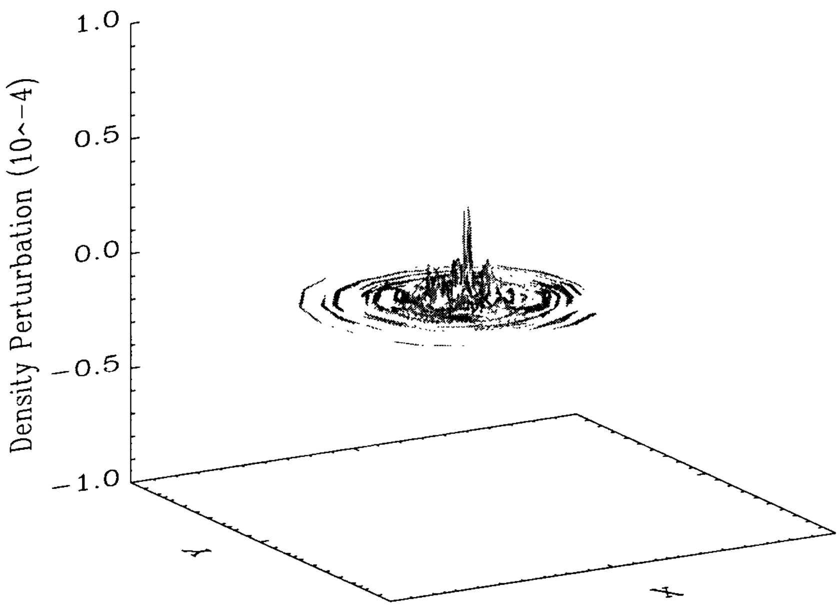

(a) Perturbed δn at $t = 0$.

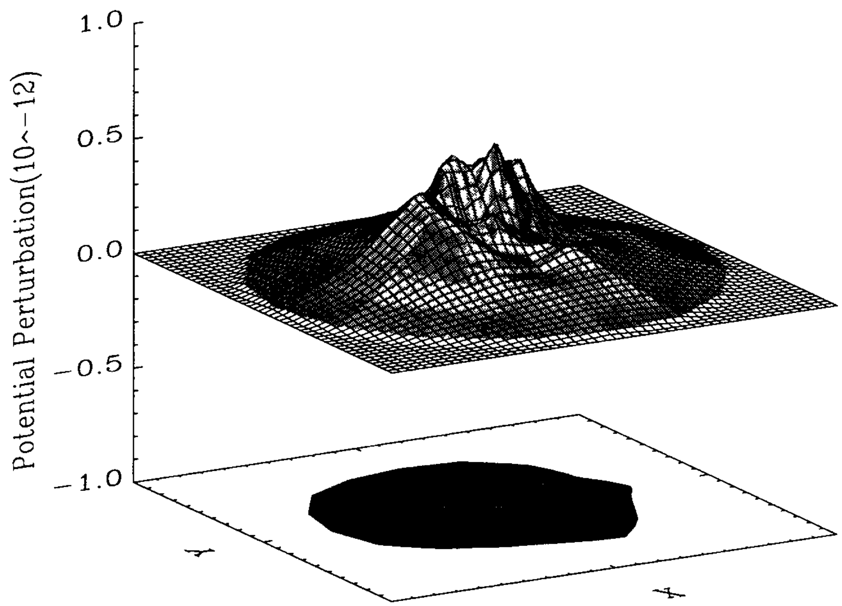

(b) Perturbed Space-Charge Potential $\delta\phi$ at $t = 0$.

- Random initial perturbation with normalized amplitudes of 10^{-4} are introduced into the system.

Nonlinear Properties of Thermal Equilibrium Beams

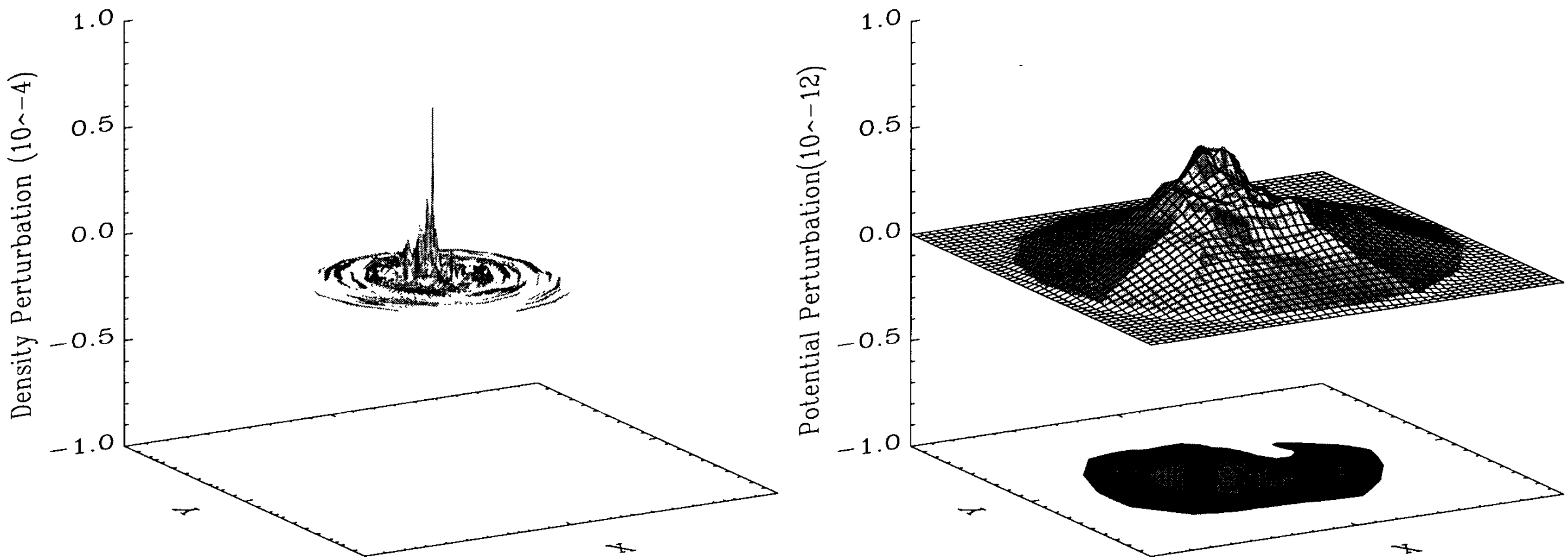

(a) Perturbed δn at $t = 500\tau_\beta$.

(b) Perturbed Space-Charge Potential $\delta\phi$ at $t = 500\tau_\beta$.

➪ The beam is propagated from $t = 0$ to $t = 500\tau_\beta$, where $\tau_\beta \equiv \omega_{\beta b}^{-1}$.

Nonlinear Properties of Thermal Equilibrium Beams

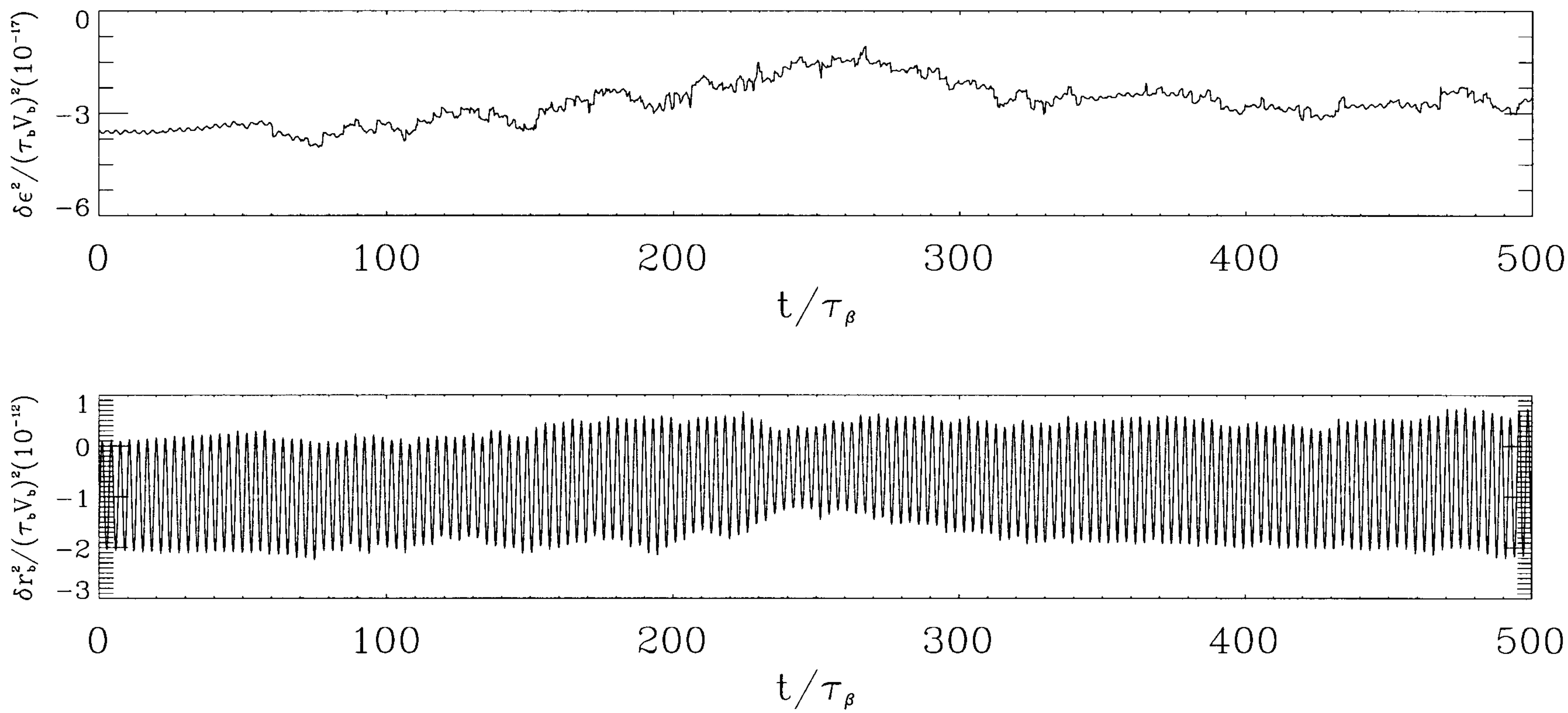

➪ Simulation results show that the perturbations do not grow and the beam propagates quiescently, which agrees with the nonlinear stability theorem for the choice of thermal equilibrium distribution function.

Surface Modes

➪ Linear surface modes for perturbations about a thermal equilibrium beam in the space-charge-dominated regime, with flat-top density profile.

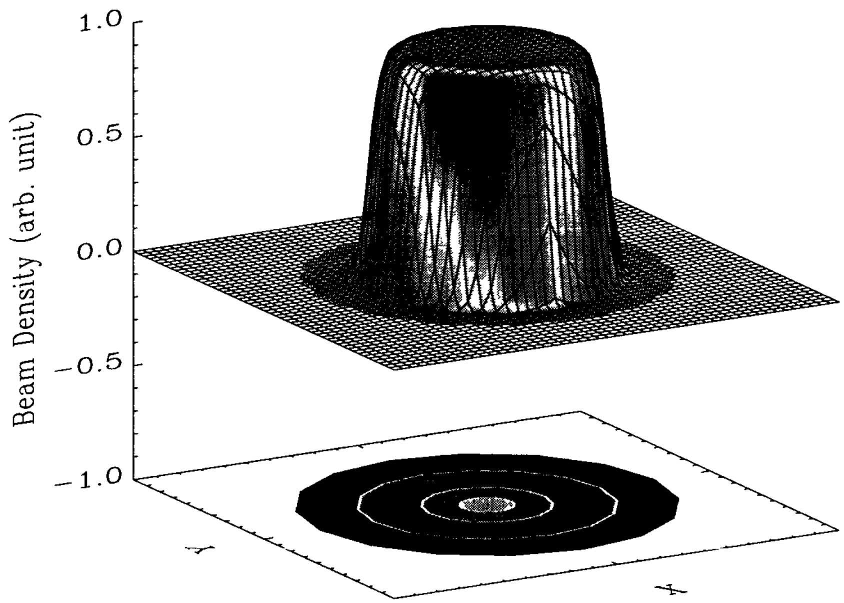

(a) Equilibrium Density

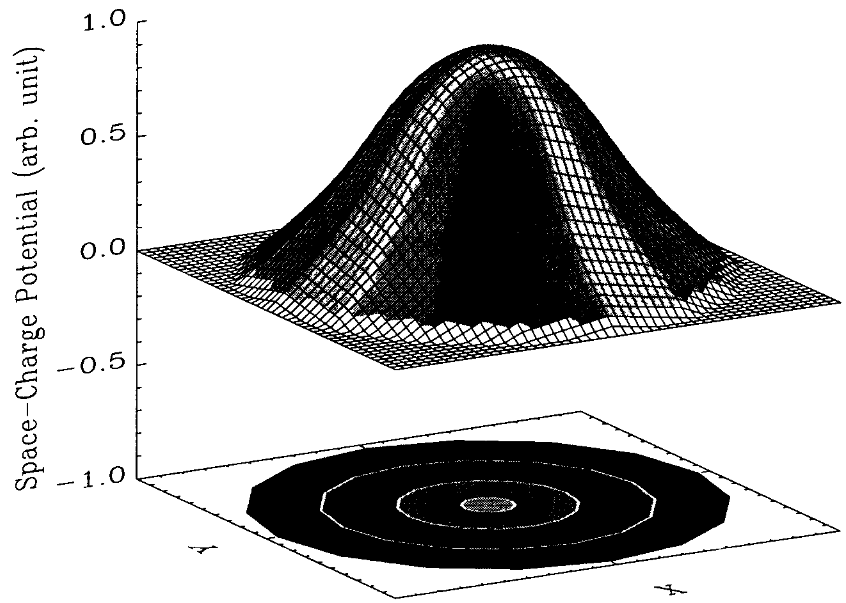

(b) Equilibrium Space-Charge Potential

Surface Modes

- These modes can be destabilized by the electron-ion two-stream interaction when background electrons are present.
- The BEST code, operating in its linear stability mode, has recovered well-defined eigenmodes which agree with theoretical predications.

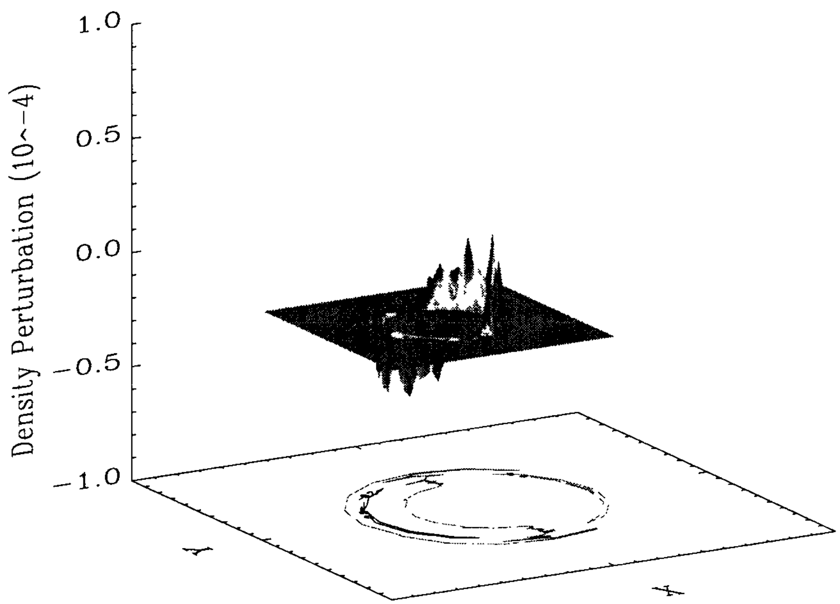

(a) Density Perturbation.

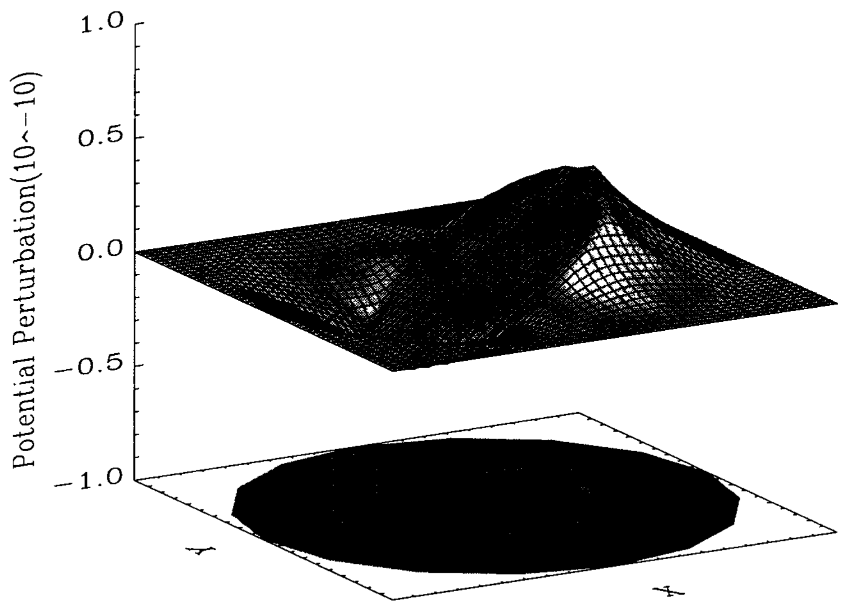

(b) Potential Perturbation.

Surface Modes

➪ For azimuthal mode number $l = 1$, the dispersion relation is given by

$$\omega = k_z V_b \pm \frac{\hat{\omega}_{pb}}{\sqrt{2}\gamma_b}\sqrt{1 - \frac{r_b^2}{r_w^2}} \tag{1}$$

where r_b is the radius of the beam edge, and r_w is location of the conducting wall. Here, $\hat{\omega}_{pb}^2 = 4\pi\hat{n}_b e_b^2/\gamma_b m_b$ is the ion plasma frequency-squared, and $\hat{\omega}_{pb}/\sqrt{2}\gamma_b \simeq \omega_{\beta b}$ in the space-charge-dominated limit with $K\beta_b c\tau_\beta/\epsilon_0 \gg 1$.

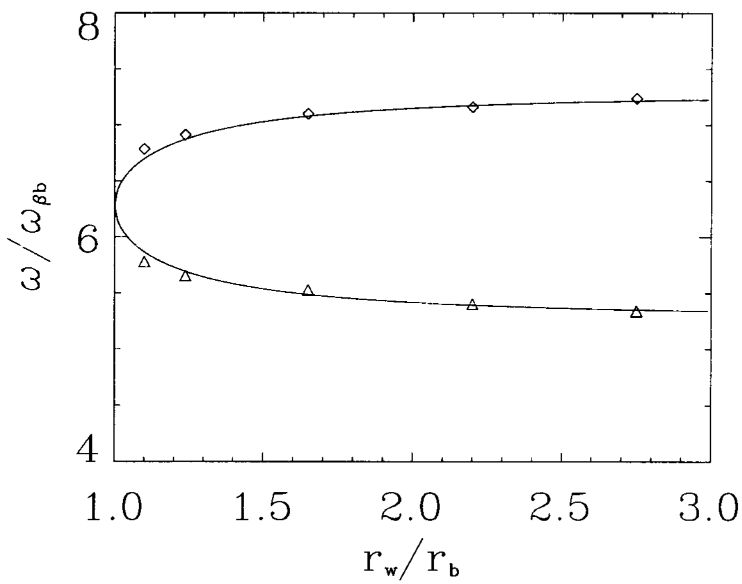

(a) $\omega/\omega_{\beta b}$ versus r_w/r_b

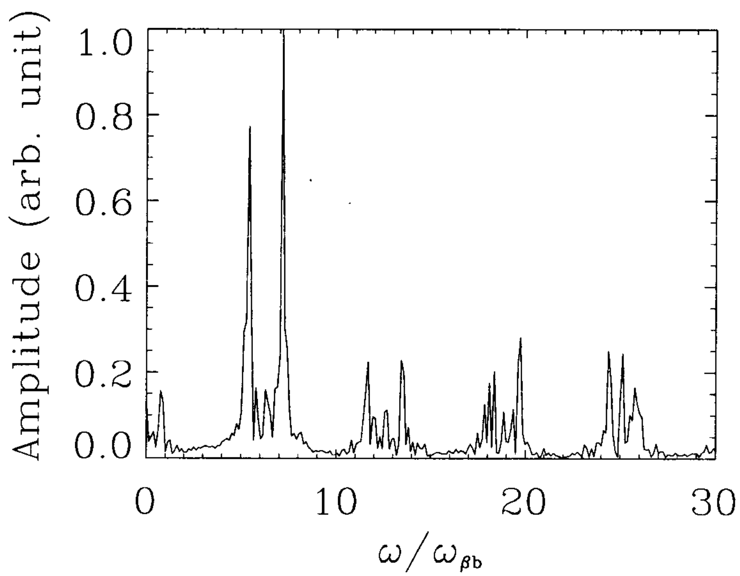

(b) Spectrum for $r_w/r_b = 2.2$

$l = 1$ Eigenmode in a Near-Gaussian Density Beam

- Generally, these is no analytical description of the eigenmodes in beams with nonuniform density profiles.
- However, numerical result shows that eigenmode is localized in the region where the density gradient is large.

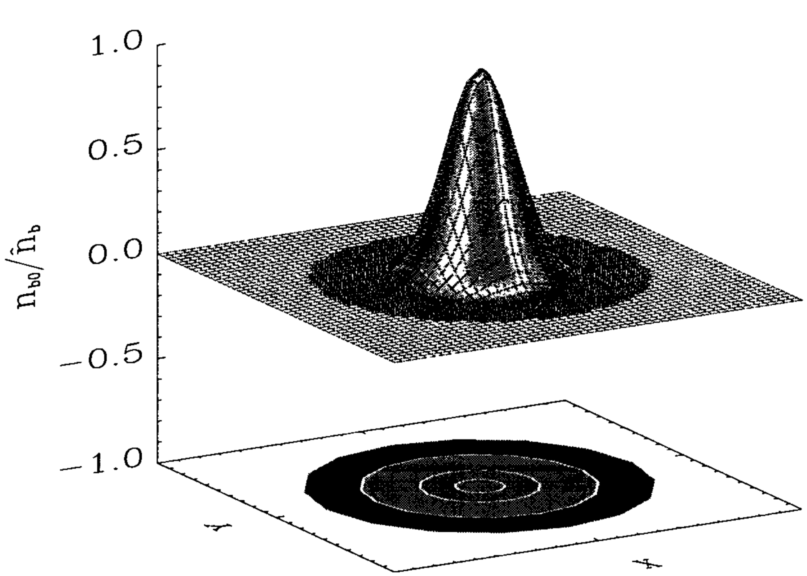

(a) Equilibrium Density Profile

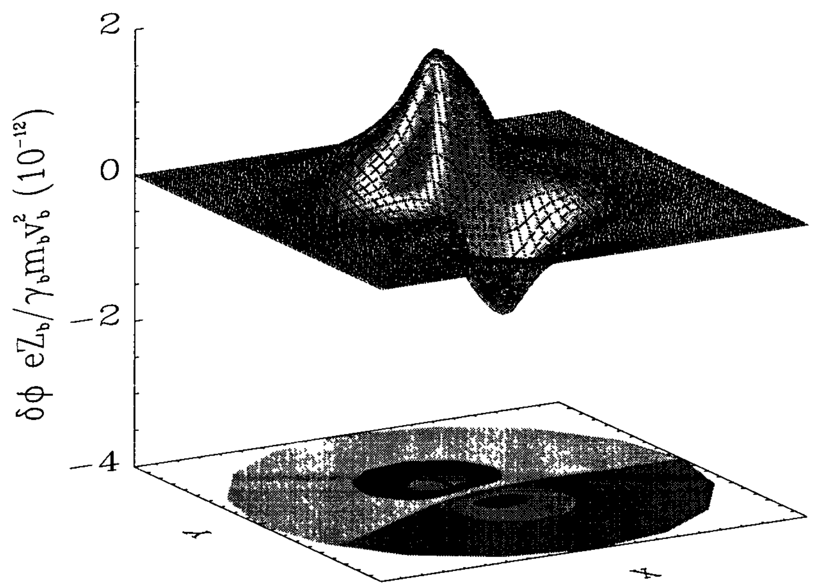

(b) Mode Structure

Electron-Proton Two-Stream Instability

- When a background electron component is introduced with $\beta_e = V_e/c \simeq 0$, the $l = 1$ "surface mode" can be destabilized for a certain range of axial wavenumber and a certain range of electron temperature T_e.

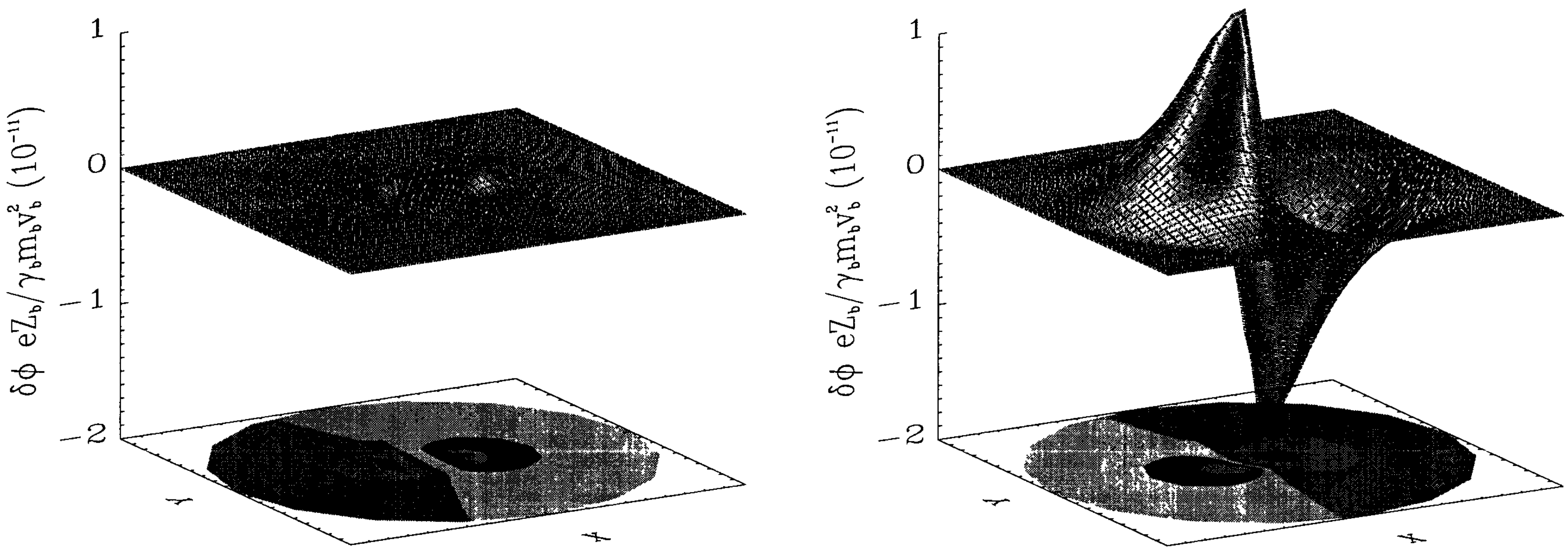

(a) $t = 0$ (b) $t = 100/\omega_{\beta b}$

Instability Growth Rate

- The $k_z V_b/\omega_{\beta b}$ and T_e/T_b dependences of the growth rate are qualitatively consistent with the analytical results obtained for uniform-density beams.

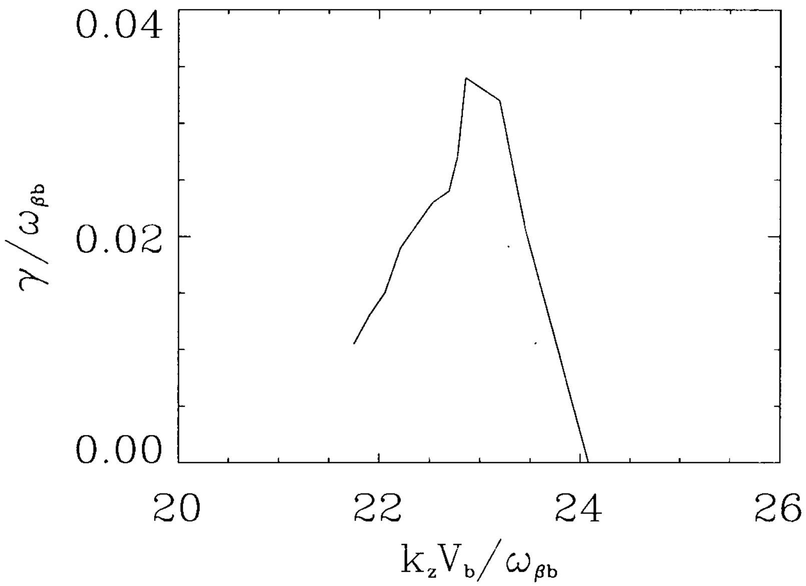

(a) γ versus $k_z V_b/\omega_{\beta b}$

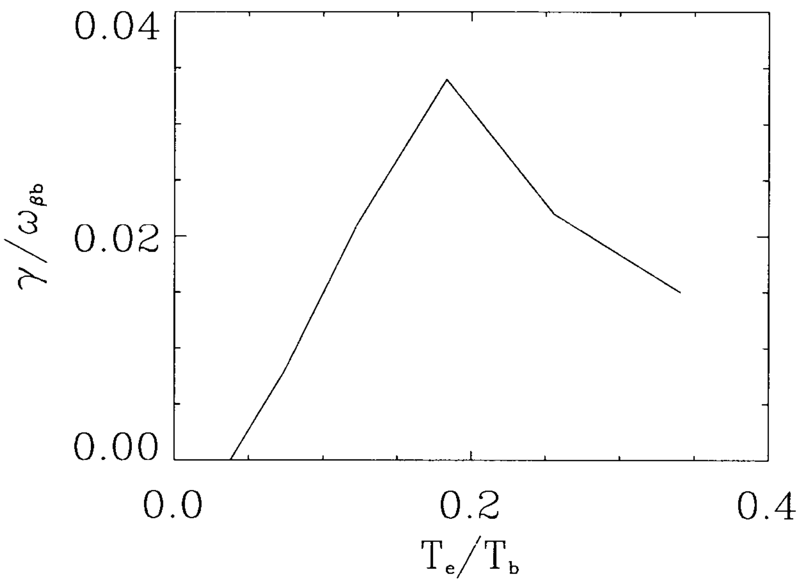

(b) γ versus T_e/T_b

- System parameters: $\hat{\omega}_{pb}^2/\gamma_b^2\omega_{\beta b}^2 = 0.1$, $T_b/\gamma_b m_b V_b^2 = 2.25 \times 10^{-6}$, and $f = \hat{n}_e/\hat{n}_b = 0.1$.

Instability Growth Rate

- ➩ $k_z V_b/\omega_{\beta b}$ dependence:
  - ❍ Only for a certain range of $k_z V_b/\omega_{\beta b}$ can the collective mode of the beam ions effectively resonate with the electrons and produce instability.
- ➩ T_e/T_b dependence:
  - ❍ For instability, electrons must physically overlap the region of the eigenmode.
  - ❍ Electrons are radially confined by the potential of the beam ions.
  - ❍ Electron temperature determines the radial extent of the electron density profile.

Cold Electrons with $T_e/T_b = 0.014$

- Electrons are relatively cold and localized in the beam center, and no instability developed over $100\omega_{\beta b}^{-1}$.

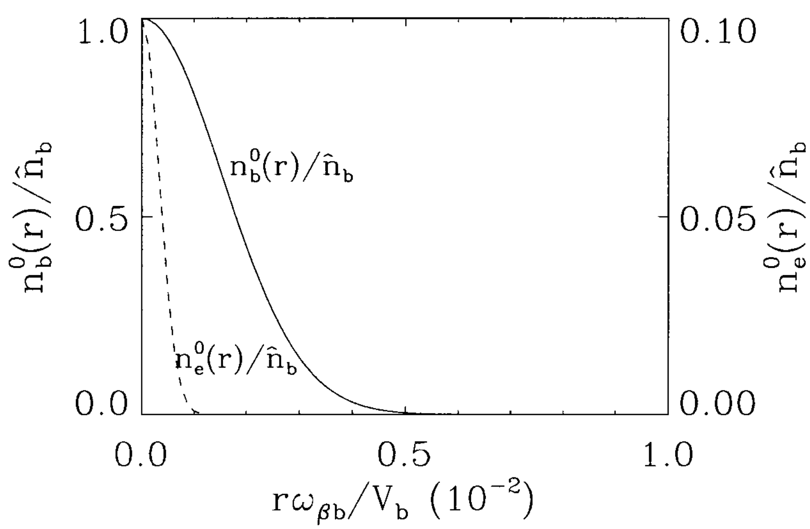

(a) Equilibrium Density

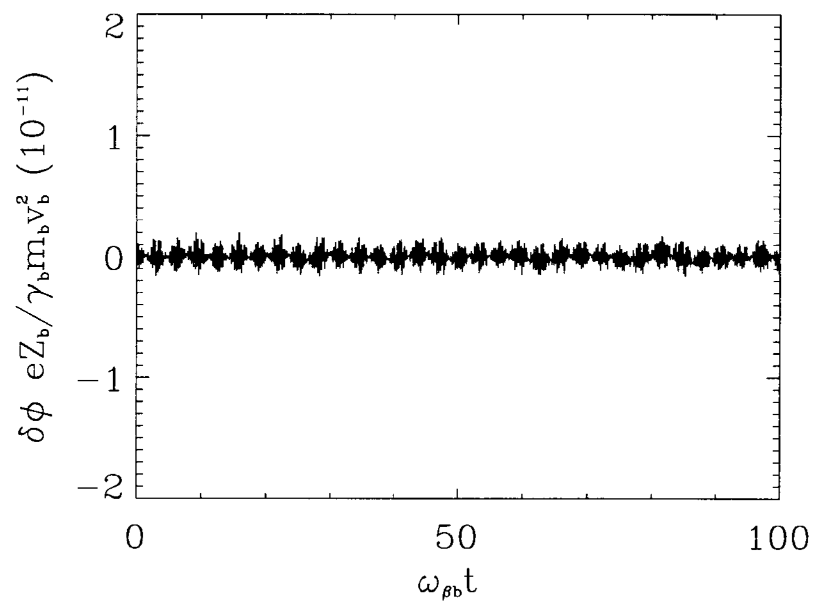

(b) Perturbation Time History

Warm Electrons with $T_e/T_b = 0.183$

- Electrons are sufficiently hot that the electron density profile overlaps that of the beam ions, and the onset of a strong e-p instability is observed.

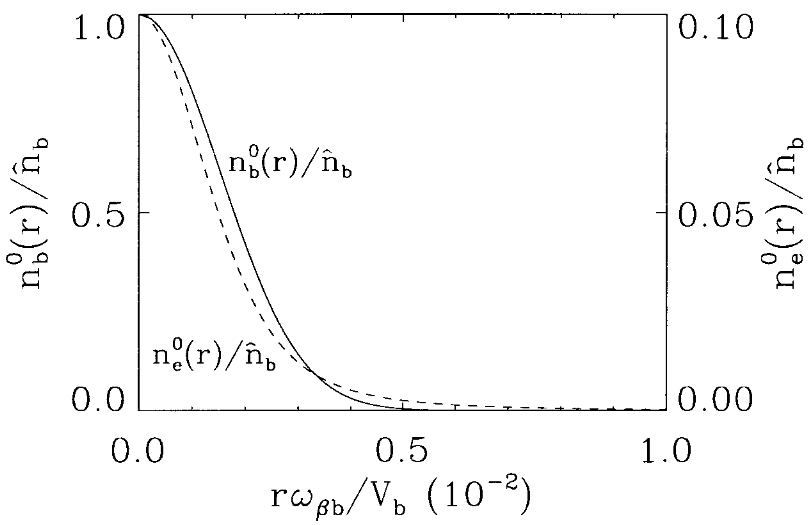

(a) Equilibrium Density

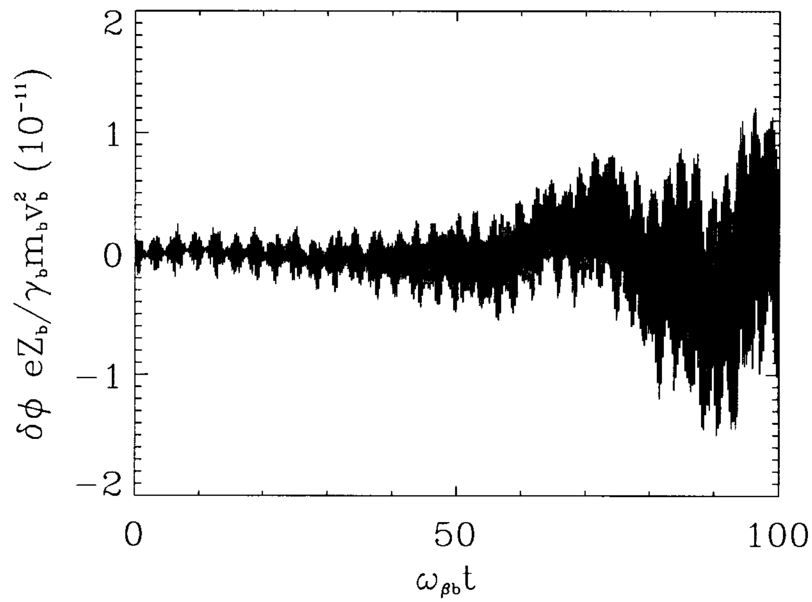

(b) Perturbation Time History

Work in Progress

- The nonlinear phase of the electron-ion two-stream instability for high-intensity beam propagation is being simulated.
- The BEST code is readily adapted to the case of periodic focusing quadrapole field or solenoidal field, and can be used to find peroidically-focused solutions.
- The BEST code is being parallelized to run on tera-scale parallel computers.

Conclusions

- A 3D multispecies nonlinear perturbative particle simulation method has been developed to study collective instabilities in intense charged particle beams described self-consistently by the Vlasov-Maxwell equations.
- Simulation results show that a thermal equilibrium ion beam in a constant focusing field is nonlinearly stable and can propagate quiescently over hundreds of lattice periods.
- For surface eigenmodes excited in a uniform-density beam, the simulation results agree well with the analytical results.
- Introducing a background component of electrons, the electron-proton (e-p) two-stream instability is observed in the simulations. Several properties of this instability are investigated numerically , and are found to be in qualitative agreement with theoretical predictions.

Conclusions

- The BEST code, a 3D multispecies perturbative particle simulation code, has been tested and applied in different scenarios.
- Simulation particles are used to follow only the perturbed distribution function and self-fields. Therefore, the simulation noise is reduced significantly.
- Perturbative approach also enables the code to investigate different physics effects separately, as well as simultaneously.
- The BEST code can be easily switched between linear and nonlinear operation, and used to study both linear stability properties and nonlinear beam dynamics.
- These features provide us with an effective tool to investigate the electron-ion two-stream instability, periodically focused solutions in alternating-gradient focusing fields, halo formation, and many other important problems in nonlinear beam dynamics and accelerator physics.

References

[1]R. C. Davidson, *Physics of Nonneutral Plasmas* (Addison-Wesley Publishing Co., Reading, MA, 1990), and references therein.

[2]T. P. Wangler, *Principles of RF Linear Accelerators* (John Wiley & Sons, Inc., New York, 1998).

[3]M. Reiser, *Theory and Design of Charged Particle Beams* (John Wiley & Sons, Inc., New York, 1994).

[4]W. W. Lee, Q. Qian, and R. C. Davidson, Physics Letters A **230**, 347 (1997).

[5]Q. Qian, W. W. Lee, and R. C. Davidson, Physics of Plasmas **4**, 1915 (1997).

[6]P. H. Stoltz, W. W. Lee, and R. C. Davidson, Nuclear Instruments and Methods in Physics Research **415**, 433 (1998).

[7]P. H. Stoltz, R. C. Davidson, and W. W. Lee, Physics of Plasmas **6**, 298 (1999).

[8]H. Qin, R. C. Davidson, and W. W. Lee, Proceedings of the 1999 Particle Accelerator Conference, in press (1999).

[9]R. C. Davidson, H. Qin, and T. -S. Wang, Physics Letters A **252**, 213 (1999).

[10]R. C. Davidson, H. Qin, P. H. Stoltz, and T. -S. Wang, Physical Review Special Topics on Accelerators and Beams **2**, 054401 (1999).

[11]P. J. Channell, Physics of Plasmas **6**, 982 (1999).

[12]R. C. Davidson, H. Qin, and P. J. Channell, Physics Letters A, in press (1999).

[13]R. C. Davidson, H. Qin, and P. J. Channell, Physical Review Special Topics on Accelerators and Beams, in press (1999).

[14]R. C. Davidson and C. Chen, Particle Accelerators **59**,175 (1998).

[15]R. C. Davidson, Physical Review Letters **81**, 991 (1998).

[16]R. C. Davidson, Physics of Plasmas **5**, 3459 (1998).

[17]D. Neuffer, E. Colton, D. Fitzgerald, T. Hardek, R. Hutson, R. Macek, M. Plum, H. Thiessen, and T. -S. Wang, Nuclear Instruments and Methods in Physics Research **A321**, 1 (1992).

[18] D. Neuffer and C. Ohmori, Nuclear Instruments and Methods in Physics Research **A343**, 390 (1994).

[19] M. A. Plum, D. H. Fitzgerald, D. Johnson, J. Langenbrunner, R. J. Macek, F. Merrill, P. Morton, B. Prichard, O. Sander, M. Shulze, H. A. Thiessen, T. -S. Wang, and C. A. Wilkinson, Proceedings of the 1997 Particle Accelerator Conference, 1611 (1997).